

Observation of the formation of a carbon-rich surface layer in silicon

H.J. Osten, M. Methfessel, G. Lippert, and H. Rucker

Institut für Halbleiterphysik, P.O. Box 409, D-15204 Frankfurt (Oder), Germany

(Received 9 June 1995)

Due to its small size, the carbon atom has a very low solubility in a silicon crystal. In spite of this, we show that carbon atoms adsorbed on top of a silicon surface readily migrate into substitutional sites below the surface, leading to a narrow layer of a highly concentrated alloy. This was demonstrated by depositing carbon on a Si (001) surface by molecular beam epitaxy and investigating the changes in the chemical environment by x-ray photoelectron spectroscopy during successive annealing steps at increasing temperatures. *Ab initio* total-energy calculations were used to interpret the measured spectra.

I. INTRODUCTION

Understanding the microscopic processes that take place during crystal growth is desirable because, by using suitable growth conditions far from equilibrium, materials can be trapped in a metastable state. For example, molecular beam epitaxy (MBE) at low temperatures,¹⁻³ rapid thermal chemical vapor deposition (RTCVD),⁴ or atmospheric pressure CVD (Ref. 5) can be used to grow silicon crystals containing some amount of carbon, even though stoichiometric SiC is the only stable compound permitted by the Si-C phase diagram.

The way in which the grown material depends on parameters such as temperature or deposition rate can usually only be determined empirically. For the Si-C system, an important quantity is the amount of carbon that can be incorporated without destroying the perfection of the crystal, and this generally seems to lie below a few percent. Carbon and silicon atoms have grossly different sizes and, therefore, substitutional C impurities in Si are surrounded by energetically unfavorable strain fields. The total energy can be reduced by a large amount if the atoms rearrange to make silicon carbide microcrystallites, a process which is easier if the carbon concentration is high. However, there have been recent indications that considerably higher concentrations can be attained under certain growth conditions.⁶⁻⁸

In the approach that we have studied previously,⁸ the key seems to be that pure carbon is deposited onto the clean Si surface by MBE without coevaporation of silicon. A pseudomorphic structure results when this is capped by silicon after a further growth interruption. We would like to distinguish between the two conceivable processes by which the crystalline structure can form, namely: (a) that the C atoms first stay on the surface, then reshuffle together with the silicon atoms from the cap; or (b) that the carbon atoms immediately move into the crystal before additional Si is put on top. Both models would seem to have problems. If the C and Si atoms do rearrange together, it is more likely that they would lower their energy by forming SiC microcrystallites. On the other hand, the equilibrium solubility of C in Si at the growth temper-

ature of 600–700 °C is extremely small⁹ and immediate diffusion into the lattice would be surprising. However, the results presented here will show that, unexpectedly, carbon atoms, in fact, move very easily from the surface into subsurface substitutional sites, building up a narrow layer with a high carbon concentration.

We thus come to an interesting conclusion concerning the ordered carbon-covered silicon (001) surface, a system which has been the subject of previous discussions.¹⁰ In brief, such a surface does not exist. At low temperatures, we find a disordered jumble of carbon clusters on top of the surface and at (moderately) higher temperatures, we find a concentrated pseudomorphic surface alloy.

The conclusions are based on x-ray photoelectron spectroscopy (XPS) measurements of carbon-containing silicon layers, during MBE growth and subsequent tempering steps. This is possible because of an unusual arrangement in our MBE system, which permits *in vacuo* and *in situ* XPS measurement directly after deposition, without the need to transfer the sample to another part of the chamber. The sample does not have to be cooled before taking the XPS spectrum, which avoids possible structural changes related to an unintended change in temperature. To interpret the measured data, we use *ab initio* density-functional calculations that simulate the emission of the core electron by a supercell containing an atom with a reduced core occupation. Although the relevant shifts in the XPS peaks are rather small (about 0.3 eV), we intend to show that this combination of experiment and theory can nevertheless lead to convincing conclusions.

II. EXPERIMENTAL AND THEORETICAL PROCEDURE

The layers were grown in a multichamber MBE system with a base pressure below 10^{-10} mbar. Silicon was evaporated from an electron-beam evaporator and carbon was supplied by a pyrolytic graphite-filament sublimation source. On a clean (2×1) reconstructed silicon

surface a 50-nm-thick Si buffer layer was grown at 600 °C. Carbon was evaporated with a low flux density after a short growth interruption (no difference was found for interruptions between 1 min and 1 h). In some cases, the layer was covered with 100-nm amorphous silicon (deposited at room temperature) to allow a calibration with secondary-ion-mass spectroscopy yielding a carbon deposition rate of approximately 0.2 ML per minute. The MBE equipment also contains the XPS tools. We employed a twin anode assembly that allows us to switch between Mg- and Al- $K\alpha$ excitation lines. The impinging angle was 30° relative to the surface normal and the spot size was about 200 μm in diameter. The emitted photoelectrons normal to the surface were recorded with a spherical analyzer. The sample was electrically grounded. The Si 2*p* peak from the MBE-grown pure silicon substrate below the carbon-containing layer was used as an internal reference in all measurements. Since the inelastic mean free path of the Si 2*p* photoelectrons with Mg- $K\alpha$ excitation in silicon is 27 Å, we only see the Si atoms in close vicinity of the carbon that we are interested in. By using the Si peak as reference, we eliminate possible artifacts caused by band bending or buildup of a surface potential.

Obtaining accurate theoretical values for core-level binding energies (CLBE) is already difficult for metals and faces additional complexities for semiconductors. We used the full-potential linear-muffin-tin-orbital method within the local-density approximation¹¹ to calculate the change in the total energy when a core electron is removed from the 1*s* state of a carbon atom. This type of treatment, while more involved computationally, includes final-state screening effects in addition to the “static” initial-state core levels in the unperturbed system.¹² We intend to compare semimetallic and semiconducting systems and expect final-state effects to play a non-negligible role. Supercells with (in most cases) 32 atoms were used to separate the excited atoms. The removed core electron was smeared out as a homogeneous background charge to permit solution of Poisson’s equation. To reduce the effect of the artificial background charge, total-energy differences were taken relative to auxiliary calculations with one electron removed from the valence band and smeared out as background, giving the energy needed to promote the core electron to the top of the valence band.

An additional problem is that the comparison to the measured core levels requires information about the reference level in the different parts of the crystal.¹³ For this, we must estimate the band lineup, which arises when one of the carbon-containing structures is on top of the silicon substrate. A reasonably realistic estimate is to line up the midgap energies.¹⁴ We transform the calculated core-level binding energies in this sense by adding one half of the calculated energy gap to the total-energy difference. Overall, the calculated core-level binding energies are shifted systematically by only about 2.5 eV (that is, by less than 1%) relative to the experimental values, despite the fact that the local-density approximation should work best for spatially slowly varying charge densities. Differences between materials are reproduced

to much higher accuracy.

There are some uncertainties in the calculated core-level binding energies. First, we can only consider simplified model structures instead of the presumably more complicated atomic arrangement in the samples. Second, we do not know the exact band lineup that the carbon-containing trial structure has relative to the silicon substrate. Third, since the local-density approximation underestimates energy gaps, screening effects to the core-level binding energy might be underestimated. In sum, we expect the calculations to be more useful as a guide to identify plausible structures, instead of a tool to pinpoint the exact geometry. We certainly expect trends (such as the dependence of the CLBE on the local volume of a C impurity discussed below) to come out correctly. In any case, we have checked that the overall conclusions do not change when other obvious prescriptions are used, such as correcting the total-energy difference, using the experimental (not calculated) band gap or lining up energy levels somewhat closer to the valence band.

III. RESULTS AND INTERPRETATION

Our starting point is a recent demonstration⁸ that one way to produce pseudomorphic layers of a Si-C alloy with high carbon concentration is to deposit about one monolayer of pure carbon on a Si (001) surface by MBE *without* coevaporation of silicon. After a further growth interruption, a Si cap layer is grown on top. Transmission electron microscopy (TEM) images showed that this procedure produces defect-free pseudomorphic layers with a width compatible to a concentration of up to 20%. As discussed in the introduction, our aim is to obtain information about the growth process by which these structures are created.

A first measurement was done to identify the XPS “fingerprint” of the pseudomorphic carbon-containing layers, as grown by the previously described method. After deposition of approximately one monolayer of carbon on the clean Si (001) surface, we obtained a C 1*s* core level binding energy of 282.8 eV. Next, a 1.5-nm-thick Si cap layer was deposited on top of the structure. The XPS spectrum obtained after this step does not differ significantly from that observed before, except for a lower signal intensity, due to the limited information depth. The temperature was kept constant at 600 °C throughout the deposition and XPS measurement steps. We conclude that the carbon-containing pseudomorphic layer is associated with a CLBE of 282.8 eV, which lies between the characteristic peaks for graphite (284.3 eV) and SiC (282.4 eV). The latter can, for example, be identified using our apparatus during imperfect high temperature *in situ* cleaning steps.¹⁵ Despite the relatively small shift relative to the SiC peak position, the 282.8-eV signal is not due to the formation of SiC microcrystallites. During the carbon deposition, we observe a typical streaky (2×1) reflection high-energy electron diffraction pattern without the additional spots which would be typical for silicon carbide cluster formation.¹⁶ In any case, forma-

tion of SiC at a temperature of 650 °C is unlikely. For example, investigations concerned with the growth of silicon carbide on Si (001), using the template technique,¹⁷ yielded a minimum formation temperature above 900 °C. Note that the line near 282.8 eV is already seen after the carbon deposition step and before growth of the Si overlayer. In principle, this single result already demonstrates the claim made in the introduction, namely, that the final carbon-containing layer already forms as soon as the carbon is deposited onto the clean Si surface.

Elaborating on this results, the second set of experiments tries to get more information on the growth process by heating the sample gradually. We first deposited approximately one monolayer of carbon on a silicon surface grown with MBE and cooled it down to room temperature. The layer was annealed *in vacuo* at 100, 200, 300, 400, and 500 °C for 40 min at each temperature, followed by further anneals at 550, 600, 650, 700, and 750 °C for 20 min at each temperature. At the end of each annealing step, we measured the C 1s XPS signal. After the initial low-temperature carbon deposition, the C 1s signal is found near 283.52 eV. Starting with the 500 °C anneal, the signal shifts to lower binding energies and saturates at a value of 282.83 eV for temperatures above 650 °C. This position is identical to the "fingerprint" identified in the first experiment. As further proof that this signal is not due to SiC, we used an additional high temperature (920 °C/15 min) anneal. After this, we measured an additional shift of 0.26 eV to a peak position typical for silicon carbide on silicon. Figure 1 shows the measured spectra for three typical temperatures. Conspicuous is the shift from a rather broad peak at 20 °C to a narrower peak at a lower binding energy as the annealing temperature is increased. Although small, the shift is clearly visible and reproducible. To show that there are really three different well-defined characteristic core binding energies,

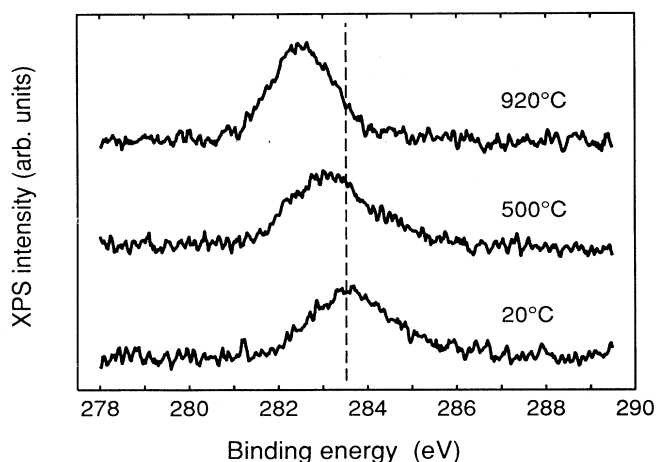


FIG. 1. XPS spectra of the C 1s state, measured after the carbon-covered Si (001) surface was annealed in steps up to the indicated temperature for each curve. With increasing temperature, the peak shifts to lower energies and becomes more narrow. The dashed line marks the position of the peak at 20 °C.

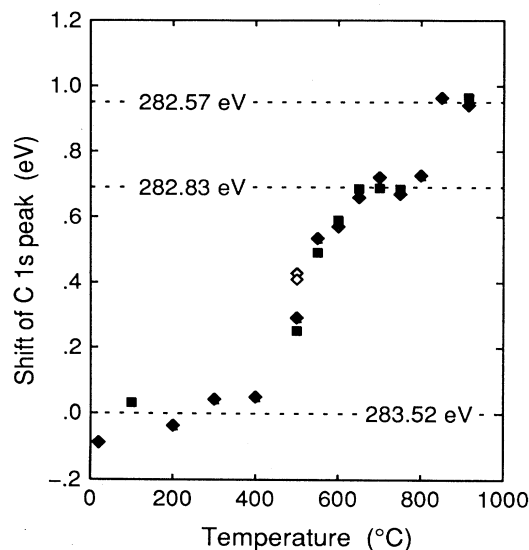


FIG. 2. Shift of the measured C 1s peak in dependence of the temperature for the last annealing step, relative to the position after deposition at room temperature. Three distinct plateaus (dashed lines) at the indicated core-level binding energies are observed. Measurements for two different samples are distinguished by squares and diamonds; open symbols indicate extra annealing steps at 500 °C for determining the energy barrier.

Fig. 2 displays the peak position against the annealing temperature. One sees that at about 500 °C, some process is initiated that stabilizes by 650 °C – 750 °C at the intermediate binding energy 282.83 eV. Further heating "ruins" the sample by forming SiC crystallites in the expected manner. Figure 2 shows closely similar values for two separate runs on different samples.

To help identify the three plateaus found for the XPS signals as a function of annealing temperature, we first compare them to established values^{15,18} for SiC, graphite, and diamond in the top part of Fig. 3. The interpretation of the high-temperature signal ($T_2 = 920$ °C) as SiC is confirmed. For the room-temperature deposition ($T_0 \approx 20$ °C), we expect a variety of carbon clusters with some bonding to the Si substrate. This agrees with the measured XPS signal in the vicinity of the graphite value, but with some shift towards SiC. The signal of main interest here, the peak at 282.83 eV for annealing temperatures near $T_1 = 650$ °C, lies between these values. The similarity of the measured signal to the SiC value suggests the formation of Si-C bonds; however, the shift shows that the chemical environment is different from that in silicon carbide. We know that pseudomorphic growth on top of the carbon-containing layer is possible and, furthermore, that the simple substitutional C impurity in Si has a lower energy than more complicated complexes.¹⁹ Therefore, good candidates are structures consisting of an arrangement of such impurities.

The lower part of Fig. 3 shows our calculated values for the reference materials SiC, graphite, and diamond and for three trial structures containing substitutional C

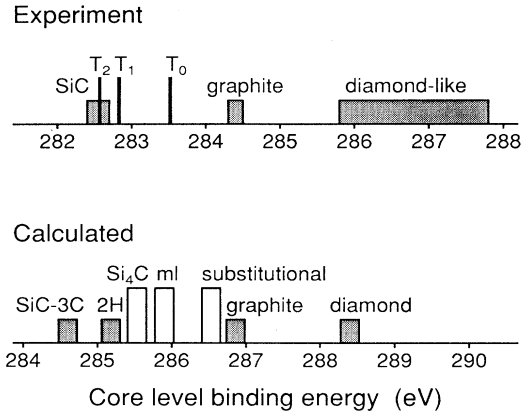


FIG. 3. Top: measured carbon 1s core-level binding peak positions at the plateaus in the annealing curve near $T_0 = 20^\circ\text{C}$, $T_1 = 650^\circ\text{C}$, and $T_2 = 920^\circ\text{C}$, and previously obtained values for SiC, graphite, and diamond/diamond-like films. Bottom: Values obtained from *ab initio* supercell calculations. Theoretical values were shifted to line up graphite, for which the uncertainty in the band-edge line up does not enter.

impurities. The first candidate is the isolated substitutional C impurity, treated in a 32-atom supercell. The second (labeled ml) is made by spreading one monolayer of carbon over two adjacent Si (001) planes without creating nearest-neighbor C-C pairs, treated in a 12-atom supercell with six (001) planes. The third is a low-energy ordered structure with stoichiometry Si_4C in a cell of 10 atoms.⁸ All three were forced to match the Si substrate and atomic positions were relaxed using a realistic Keating model⁸ prior to the *ab initio* calculation.

As discussed above, exact identification of the structure causing the T_1 signal by comparing theory and experiment is overambitious. Nevertheless some clear trends emerge. All three trial structures have a chemical environment similar to SiC, in that the carbon atom is tetrahedrally surrounded by four Si atoms. However, the calculated core-level binding energies are different by more than 1 eV. For the isolated substitutional impurity, the value is similar to that of graphite and lies too high to be considered as the source of the T_1 signal. For the structures with more carbon, the binding energy lies slightly above that of SiC and is compatible with the measured peak position. As mentioned, this should not be overinterpreted; specifically, the calculated results for SiC cannot be directly compared to the measured value, because of the many possible modifications which, moreover, have different band gaps. (The difference in the cubic and hexagonal SiC CLBE is due to the smaller band gap in the cubic modification, which enters via the band lineup model used here.) But it seems safe to conclude that a substitutional structure is a suitable model for the measured system, if we can understand why some of these have core-level binding energies that lie closer to that of SiC than others.

We have to explain why the various substitutional structures and SiC lead to different values of the CLBE,

even though they have a similar nearest-neighbor environment of the carbon atom. In silicon carbide, the charge is transferred to the carbon atom, raising the electrostatic potential and reducing the C 1s core-level binding energy. Thus, we associate the shifts of the CLBE relative to SiC mainly with the degree to which the much smaller C volume can be accommodated in the different structures. Stretching the C atom to fill a larger volume causes an overall decrease of the electron density around it. This lowers the electrostatic potential and increases the CLBE. Compared to the substitutional impurity, the embedded monolayer structure and Si_4C have carbon volumes much closer to that in SiC. As a very rough measure, we can assign to each Si atom the same volume as it has in the pure crystal (133 a.u.³) and determine the volume left to the carbon atom in each structure. For the used geometries of SiC, Si_4C , the embedded monolayer, and the impurity, we obtain about 3, 39, 52, and 133 a.u.³, respectively, compared to the atomic volume in diamond of 38 a.u.³. Despite the obvious defects of this definition, one sees that the carbon is stretched by a much larger amount in the structures with a higher CLBE. We are left with the following general argument: the substitutional carbon atoms will tend to reduce the total energy of the crystal by arranging in a way that permits maximal relaxation towards a small carbon volume. This increases the electron density near the carbon atom, which pushes up the core-level binding energy. Thus, the substitutional structures showing a CLBE only slightly above that of SiC are exactly those arrangements that have a low total energy.

IV. FURTHER EVALUATION OF THE XPS SPECTRA

Based on the previous discussion, we interpret the seemingly continuous shift of the XPS peak as the temperature varies from 20 to 650 °C, as due to changes in the intensity of two subpeaks, which are associated with adsorbed carbon clusters and substitutional subsurface carbon. This is confirmed by the change in line shape; starting with a symmetrical line at room temperature, we pass through a region where the line is significantly asymmetric before it becomes symmetric again after the 650 °C anneal. Each spectrum can be deconvoluted as a sum of two subpeaks fixed at the positions for room temperature and 650 °C (Fig. 4), which reproduces the observed asymmetry very well. Let c_0 and c_1 be the normalized integrated signal intensities for the first and second subpeak, which we interpret as the relative amount of carbon in each phase. At the fixed temperature $T=500^\circ\text{C}$, we performed several measurements as a function of annealing time t . The results fit well to the relation

$$c_0(t) = \exp(-t/\tau) \Rightarrow c_1(t) = 1 - \exp(-t/\tau),$$

with $\tau=85$ min. Assuming $c_0(t)$ obeys an exponential time dependence at the other annealing temperatures also, we can estimate the time constant $\tau(T)$ from the single measurement done there, giving values obeying

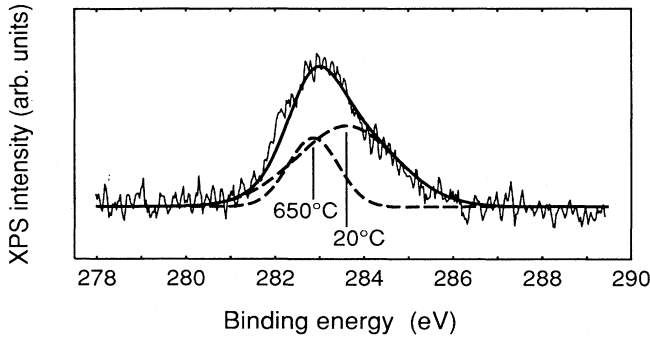


FIG. 4. Example for the deconvolution of the carbon signal (here for the spectrum obtained after the 500 °C anneal) into a sum of two peaks associated with the low (20 °C) and intermediate (650 °C) temperature structures.

$$1/\tau(T) \propto \exp(-E/kT),$$

with $E = 0.6 \pm 0.1$ eV. This energy can be viewed as the barrier for carbon atoms to migrate from the surface into subsurface sites. It is considerably smaller than the activation energy for diffusion in the bulk⁹ of about 3 eV.

As a final point in the interpretation of the results, we exploit the surface-sensitive property of the XPS technique to estimate the depth to which the C atoms move into the Si crystal. The x-ray photons penetrate deep into the substrate, but the emitted electrons are scattered with an inelastic mean free path of $\lambda=24$ Å in silicon, for C 1s electrons under Mg-K α excitation.²⁰ Of the electrons emitted at a depth d , only the fraction $\exp(-d/\lambda \sin \Theta)$ reach the surface and can be detected, where Θ is the electron take-off angle relative to the sample surface (in our case $\Theta=90^\circ$). For simplicity, we consider the case that the total amount of deposited carbon is distributed homogeneously over a layer of thickness D near the surface. The total XPS intensity then obeys

$$I(D) \propto \frac{\lambda \sin \Theta}{D} \left[1 - \exp\left(-\frac{D}{\lambda \sin \Theta}\right) \right].$$

For a given initial carbon coverage, this can be used to calculate the reduction in XPS intensity as a function of the concentration $c_C \propto 1/D$. Assuming an initial coverage of one monolayer carbon, spreading this over 100 layers of the silicon lattice (corresponding to the formation of an alloy with 1% carbon) would reduce the C 1s XPS intensity to one sixth of the initial value. Even a concentration of 5% would lead to a decrease of about 40%. In contrast, throughout the whole annealing procedure, we have found that the ratio of the integrated C 1s and Si 2p intensities remained constant to within a mean deviation of 10%. Thus, our measurements are compatible with a carbon concentration in the neighborhood of 15 – 20 % but exclude a substantially lower concentration in the surface layer.

V. CONCLUSIONS

Altogether, our experimental and theoretical results for annealing experiments on a carbon-covered Si (001) surface lead to the following conclusions. Carbon atoms deposited on silicon tend not to stay on the surface, but instead readily migrate into the crystal. There are strong indications that they occupy substitutional sites. The energy barrier of approximately 0.6 eV hereby is much smaller than that for diffusion in the bulk. The carbon atom stays close to the surface, forming an alloy with a carbon concentration above 10–20 %. We point out that recent calculations based on an empirical many-body potential²¹ predict that the interaction of the defect stress around a carbon impurity with the free surface can enhance the solubility, as well as the diffusion by a large factor. Both predictions are in very good agreement with our present results.

¹ A. R. Powell, K. Eberl, B. A. Ek, and S. S. Iyer, *J. Cryst. Growth* **127**, 425 (1993).
² H. J. Osten, E. Bugiel, and P. Zaumseil, *Appl. Phys. Lett.* **64**, 3440 (1994).
³ K. Eberl, S. S. Iyer, J. C. Tsang, M. S. Goorsky, and F. E. LeGoues, *J. Vac. Sci. Technol. B* **10**, 934 (1992).
⁴ J. L. Regolini, F. Gisbert, G. Dolino, and P. Boucaud, *Mater. Lett.* **18**, 57 (1993).
⁵ Z. Atzmon, A. E. Bair, E. J. Jaquez, J. W. Mayer, D. Chandrasekhar, D. J. Smith, R. L. Hervig, and McD. Robinson, *Appl. Phys. Lett.* **65**, 2559 (1994).
⁶ A. R. Powell, K. Eberl, F. E. LeGoues, B. A. Ek, and S. S. Iyer, *J. Vac. Sci. Technol. B* **11**, 1064 (1993).
⁷ J. Kouvetakis and M. Todd, *Appl. Phys. Lett.* **65**, 2960 (1994).
⁸ H. Rücker, M. Methfessel, E. Bugiel, and H. J. Osten, *Phys. Rev. Lett.* **72**, 3578 (1994).
⁹ G. Davies and R. C. Newman, in *Handbook on Semiconductors*, edited by T.S. Moss (Elsevier, New York, 1994), p. 1557.
¹⁰ T. Halicioglu, *Thin Solid Films* **237**, 22 (1994);

Y. Miyamoto, *Phys. Rev. B* **49**, 1947 (1994).
¹¹ M. Methfessel, C. O. Rodriguez, and O. K. Andersen, *Phys. Rev. B* **40**, 2009 (1989).
¹² M. Methfessel, D. Hennig, and M. Scheffler, *Surf. Rev. Lett.* **2**, 197 (1995).
¹³ W.-X. Ni and G. V. Hansson, *Phys. Rev. B* **42**, 3030 (1990).
¹⁴ J. Tersoff, *Phys. Rev. Lett.* **56**, 2755 (1986).
¹⁵ G. Lippert, Ph.D. thesis, Munich, 1995.
¹⁶ J. P. Becker, R. G. Long, and J. E. Mahan, *J. Vac. Sci. Technol. A* **12**, 174 (1994).
¹⁷ M. Kitabatake, M. Deguchi, and T. Hirao, *J. Appl. Phys.* **74**, 4438 (1993).
¹⁸ F. Fujimoto and K. Ogata, *Jpn. J. Appl. Phys.* **32**, L420 (1993); K. Harshavardha, R. S. Yalamanchi, and L. K. Rao, *Appl. Phys. Lett.* **55**, 351 (1989); *Handbook of X-Ray Photoelectron Spectroscopy*, edited by Jill Chastain (Perkin Elmer, Eden, Minnesota, 1992).
¹⁹ J. Tersoff, *Phys. Rev. Lett.* **64**, 1757 (1990).
²⁰ S. Tanuma, C. J. Powell, and D. R. Penn, *Surf. Interface Anal.* **17**, 911 (1991).
²¹ J. Tersoff, *Phys. Rev. Lett.* **74**, 5080 (1995).